Enhanced uniaxial anisotropy and two-step magnetization process along the hard axis of polycrystalline NiFe/NiO bilayers

T. Zhao, H. Fujiwara, K. Zhang, C. Hou, and T. Kai
Center for Materials for Information Technology, University of Alabama, Tuscaloosa, Alabama 35487-0209
(Received 4 January 2001; revised manuscript received 22 August 2001; published 13 December 2001)

Polycrystalline NiFe(10 nm)/NiO(1–8 nm) exchange-coupled bilayers show enhanced uniaxial anisotropy but no unidirectional anisotropy. Meanwhile, a two-step magnetization process was observed along the hard direction. These two phenomena cannot be simultaneously understood using the models for ferromagnetic/antiferromagnetic bilayers, in which a parallel alignment or a random distribution of the easy axes of antiferromagnetic grains is assumed. Therefore, a model, supposing a preferential distribution of the easy axes of antiferromagnetic grains, is proposed for understanding the mechanism of these phenomena.

DOI: 10.1103/PhysRevB.65.014431 PACS number(s): 75.70.Ak

I. INTRODUCTION

Exchange-coupled [ferromagnet (F)]/[antiferromagnet (AF)] bilayers have been intensively studied in recent years[1,2] because of their underlying physics and applications in the magnetic recording industry: for example, the pinned layer in spin-valve structure[3] and the soft underlayer in perpendicular media. The F/AF bilayer exhibits interesting properties, including exchange bias and enhanced coercivity, when it is cooled down from a relatively high temperature under a static magnetic field. The easy axis and/or the pinned direction of the bilayer are determined by the magnetization direction of the ferromagnetic layer during the cooling. It is generally recognized that the magnetic properties of the bilayers are determined by F/AF interfacial exchange coupling which is related to the AF spin configuration at the interface. Much fundamental research has been devoted to explaining the origin and amplitude of the exchange bias,[4–9] assuming a bilayer with single-crystalline AF layer and various interfacial conditions. It is proved that locally uncompensated interfacial AF spins are essential for the appearance of the exchange bias[7,8] and the atomic-scale interface roughness[4] and the fanning spin structures in the AF layer[6,9–11] can strongly affect the amplitude of the effective exchange coupling. For bilayers with polycrystalline AF layer, phenomenological approaches were proposed in the Fulcomer-Charap model[12] (FC model) and its extensions.[13–15] The F magnetic layer is assumed to couple with a assembly of AF grains with partially compensated interface, and both the F/AF exchange coupling and the easy axis of the AF grain may vary from grain to grain. The distribution of interfacial exchange coupling, which is related to the grain size and interface roughness, gives rise to the coexistence of the exchange bias and enhanced coercivity. An individual AF grain may contribute to the exchange bias or the enhanced coercivity depending on the ratio of the interfacial exchange coupling and the volume anisotropy of the AF grain. Another important issue in the polycrystalline F/AF layers is the distribution of the easy axes of the AF grains, which can affect both the characteristics and the amplitude of the effective anisotropy of the bilayers. In the FC model, the easy axes of AF grains are all assumed parallel to the pinned direction[12] and, in the extended models, they are assumed randomly distributed to explain a nonvanishing rotational hysteresis on the torque curve under a high magnetic field[15] and a constant frequency excitation in ferromagnetic resonance (FMR) experiments.[13,16] For the AF grains contributing to the exchange bias, the distribution of easy axes may not affect the characteristics of the anisotropy since both parallel and random distributions give a unique pinned direction, usually parallel to the applied field direction during the fabrication. It is likely that the easy axis distribution plays a more visible role for the AF grains contributed to the coercivity because their spins can switch following the switching of the F moment. In the present work, the magnetic properties of the NiFe/NiO bilayers were studied, in which the NiO layers were made relatively thin so that all the AF grains contribute to the coercivity and no exchange bias appears. In addition to the enhanced coercivity, a strong uniaxial anisotropy and a two-step magnetization process along the hard direction were observed. Both of these phenomena can be ascribed to a preferential distribution of the AF easy axes.

II. RESULTS AND DISCUSSION

The Si(110)/Ta(5 nm)/NiO(x nm)/NiFe(10 nm)/Ta(5 nm) ($x=0-8$) films were prepared by dc/rf magnetron sputtering under an argon atmosphere (5.0 mTorr). The base pressure of the chamber is about 2.0×10^{-7} Torr. An external magnetic field of 150 Oe has been applied parallel to the film surface during the sputtering. The crystal structures were checked by x-ray diffraction (XRD), using Cu $K\alpha$ radiation. It shows that the polycrystalline NiO layer has a single NaCl-type fcc phase with a combined (111) and (200) out-plane texture structure (the $\langle 111\rangle$ or $\langle 200\rangle$ direction tends to orientate perpendicular to the film plane) and NiFe has a fcc phase with a dominant (111) out-plane texture (see Fig. 1). This implies that the surface of the NiO grain at the interface may be composed of fine facets corresponding to the (111) and (200) crystal planes of NiO.[17]

The magnetic properties of the samples were characterized using a vibrating sample magnetometer (VSM) and a high-sensitivity homemade torque meter.[18] The easy-axis coercivity increases monotonically with the increase of NiO thickness (t_{NiO}) (see Fig. 2). For the films with $t_{NiO}=1$ and

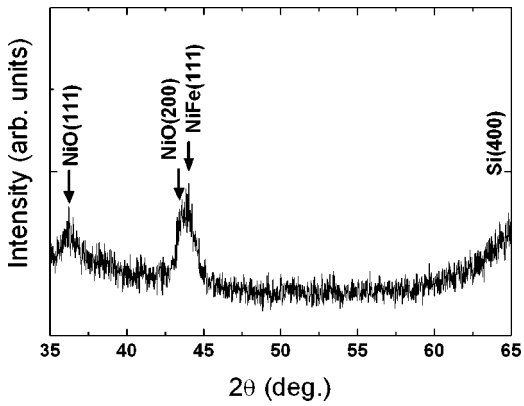

FIG. 1. X-ray spectra of a Si/Ta (5 nm)/NiO(7 nm)/NiFe(10 nm)/Ta(5 nm) multilayered sample, using Cu $K\alpha$ radiation.

2 nm, the coercivity is about 1–2 Oe and the anisotropy field around 5–6 Oe [see Fig. 4(a)], similar to the single-layer Permalloy reference sample ($x=0$) (coercivity is 1.2 Oe and anisotropy field 5.1 Oe). This can be ascribed to the so-called dead layer, a very thin NiO layer (1–2 nm) that does not show antiferromagnetic ordering due to the discontinuity and/or interfacial diffusion.[19] From $t_{NiO}=3$ nm to 8 nm, the coercivity increases monotonically up to two orders of magnitude larger than that of the sample with $t_{NiO}=1$ nm while the hysteresis loops are still symmetric, no loop shift. It is often observed in exchange-coupled F/AF bilayers that the coercivity increases with increasing AF layer thickness and reaches a peak value around the onset of the exchange bias.[14,20,21] Under a zero-temperature coherent rotation approximation, the condition for the onset of exchange bias is $r=J_{F\text{-}AF}/(2K_{AF}t_{AF})<0.5$, where $J_{F\text{-}AF}$ is the interfacial exchange coupling energy per unit area, K_{AF} the anisotropy constant of the AF layer, and t_{AF} the AF layer thickness.[15] If $r>0.5$, the AF spins can follow the switching of the F moment, giving an enhanced coercivity and no loop shift.

The torque curves of samples with different t_{NiO} in a field high enough to reach the saturated state are given in Fig. 3. The torque curves with 180° symmetry, consistent with the symmetric hysteresis loops, indicate an enhancement of the uniaxial anisotropy rather than the generation of unidirectional anisotropy usually observed in exchange-biased films

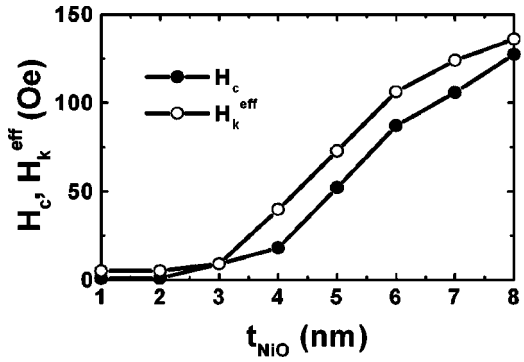

FIG. 2. Dependence of the easy-axis coercivity (H_c) and the effective anisotropy field H_k^{eff} on the thickness of NiO layer. The line is a guide to the eyes.

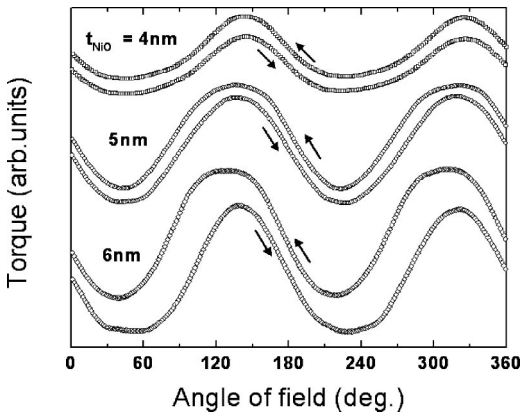

FIG. 3. Torque curves of NiFe/NiO bilayers with different NiO thickness. The torque was measured in an external field of 600 Oe and in an angle range from $-180°$ to 540°.

with thicker NiO layers. This can also be ascribed to $r>0.5$. The nonvanishing rotational hysteresis at high magnetic field is due to the retardation of the mean active easy direction (AED) of the NiO layer with respect to the magnetization of the NiFe layer, where the AED of a uniaxial AF grain is defined as one of the easy directions that is closer to the direction of the net surface moment of the grain.[15] For a film with a simple uniaxial anisotropy, the torque amplitude per unit volume is equal to the anisotropy constant (K_u) and the anisotropy field (H_k) can be expressed as $2K_u/M_s$. Here we try to extend this concept to evaluate the uniaxial anisotropy of bilayers. In the bilayers, if regarding the observed torque curves as being just a superposition of the contributions from a uniaxial part and an isotropic part (a constant shift part) phenomenologically, we can get a so-called effective anisotropy constant (K_u^{eff}) by subtracting the torque amplitude and the isotropic part and calculate the effective anisotropy field ($H_k^{eff}=2K_u^{eff}/M_s$). The quick increase of H_k^{eff} with the increase of t_{AF} (see Fig. 2) implies that the enhanced uniaxial anisotropy originates from the AF layer through the interlayer coupling. With increasing t_{NiO}, the shapes of the magnetization curves along the hard magnetization direction also change drastically. In the samples with t_{NiO} larger than 3 nm, two-step magnetization curves were observed along the hard direction [see Figs. 4(b) and 4(c)]. Hysteresis curves of similar shapes can be found in the films with biaxial anisotropy[22,23] and the small thin-film elements with vortex domain structure.[24,25] However, for the bilayers under investigation, these conditions are not satisfied so that the two-step magnetization process must come from the AF grains with distributed easy axes.

For a better understanding of the magnetic switching behaviors, a micromagnetic simulation was implemented. The simplest approach to this problem is to assume that the ferromagnetic layer have a weak induced anisotropy where magnetic moments rotate coherently during the magnetization process and that the antiferromagnetic layer consists of grains with randomly distributed easy axes.[13,15] However, with this assumption, we only get weak uniaxial anisotropy and enhanced coercivity. The coercivity increases dramatically with the increases of t_{AF} while the uniaixal anisotropy

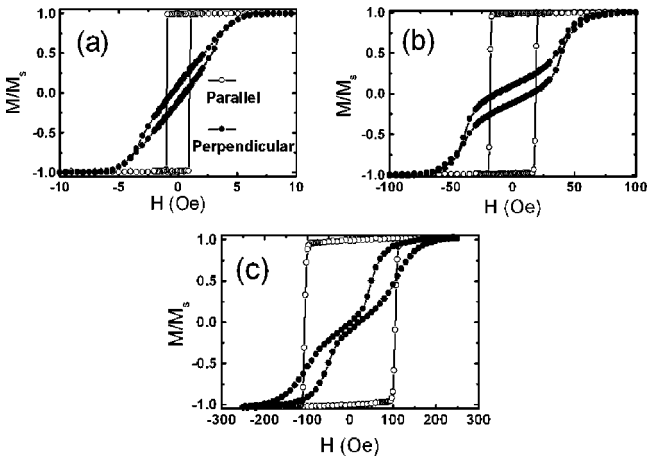

FIG. 4. Hysteresis loops along easy and hard directions with t_{NiO} of (a) 2 nm, (b) 4 nm, and (c) 7 nm measured using a VSM. The samples were saturated along the easy direction before measuring the hard-axis loop.

is kept at the same order of magnitude as the single NiFe film. The strong uniaxial anisotropy and the two-step magnetization process cannot be simulated. A natural way to introduce a strong uniaxial anisotropy depending on t_{AF} is to assume a preferential distribution of easy axes of AF grains along the magnetic field direction during the sputtering. Although it is unclear whether the uniaxial anisotropy component comes from a macrostress or an in-plane textured structure, the resulted symmetry break can give rise to a preferential distribution of easy axes as illustrated in Fig. 5. The angle θ_0 is employed to characterize this distribution; for example, θ_0 is zero for a random distribution and π for perfect parallel alignment of the easy axes. The total energy of such a system can be expressed as

$$E_{total}=\int_{-\pi/2}^{\pi/2}[J_{F\text{-}AF}\cos(\beta-\phi-\alpha_\phi)+K_{AF}t_{AF}\sin^2\alpha_\phi]f(\phi)d\phi-K_Ft_F\sin^2\beta+M_Ft_FH\cos(\psi-\beta). \quad (1)$$

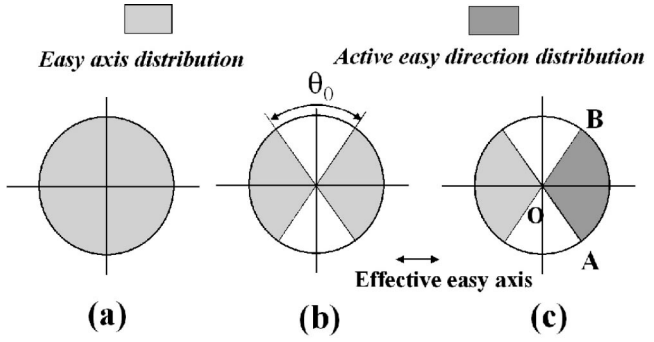

FIG. 5. Illustration of different types of distributions of easy axes and active easy directions: (a) random distribution, (b) preferential distribution, and (c) as-deposited state, assuming the sample is deposited with the applied field pointing to the right and a ferromagnetic coupling between the F moment and the AF spins.

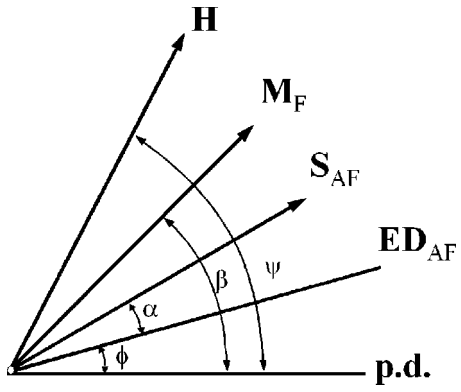

FIG. 6. Schematic of the angles used in Eq. (1). For the definition of the symbols, see the corresponding part in the text.

The first term in Eq. (1), the integration, is the summation of the interfacial exchange energies between the F layer and the AF grains and the anisotropy energies of the AF grains, the second term the anisotropy energy of the F layer, and the last term the Zeeman energy due to the interaction between the F moment and the external field. As illustrated in Fig. 6, ϕ is the angle between the easy direction of the AF grain (ED_{AF}) and the pinning direction (p.d.) which is usually parallel to the applied field direction during the film fabrication, β the angle between the F moment (M_F) and the pinning direction, α the angle between the net surface moment of the AF grain (S_{AF}) and ED_{AF}, and ψ the angle between the external field (H) and the pinning direction. K_F, M_F, and t_F are the anisotropy constant, the magnetization, and the thickness of the F layer, respectively. $f(\phi)$ is the distribution function, which gives the probability for the ED_{AF} to orient along a certain direction. $f(\phi)$ may vary in different samples. For an idealized preferential distribution as shown in Fig. 5(b), we have $f(\phi)=1/(\pi-\theta_0)$ when $-\pi/2+\theta_0/2<\phi<\pi/2-\theta_0/2$ and $f(\phi)=0$ when $\phi<-\pi/2+\theta_0/2$ or $\phi>\pi/2-\theta_0/2$. Since the AF layer is relatively thin, we have assumed that the spins in each AF grain behave coherently throughout its thickness, which means that the relative configuration of AF sublattice spins inside a AF grain is kept the same during the magnetization process so that each AF grain behaves like one spin with a certain anisotropy and magnetic moment. We have also assumed a coherent rotation of magnetization in the F layer, making β independent of ϕ. However, α differs for different ϕ because AF grains with different easy axis orientations may behave differently. In Eq. (1), we use α_ϕ instead of α, indicating that α is a function of ϕ. The hysteresis loops and the torque curves are calculated by tracing the local minima of E_{total} with respect to β and α_ϕ's for varying amplitude or direction of the magnetic field.

With the assumption of the preferential distribution of easy axes of AF grains, the strong uniaxial anisotropy consistent with the experimental results can be deduced. Figure 7 shows the calculated H_k^{eff}, using the same definition as in Fig. 2, which increases monotonically with the increase of t_{AF}. If considering the dead layer (about 2 nm) in the real sample, the calculated results quantitatively agree with the measured values. The value of $J_{F\text{-}AF}$ used in the calculation was derived from the initial susceptibility of the NiFe/NiO bilayers with a thick NiO layer, which could be an underestimate because the interlayer coupling could be weaker for larger AF grains. Then the K_{AF} was estimated by measuring

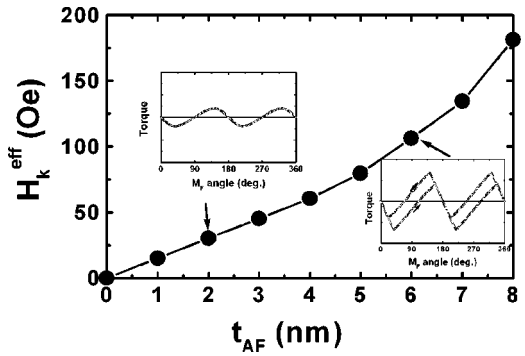

FIG. 7. Simulated dependence of H_k^{eff} on the thickness of AF layer by calculating the torque curves using the following $J_{F\text{-}AF}=0.25$ erg/cm^2, $K_{AF}=3.0\times10^5$ erg/cm^3, $M_s^F=800$ emu/cm^3, $t_F=10$ nm, and $\theta_0=\pi/3$. It shows the same tendency as the measured torque. The insets are calculated torque curves for $t_{AF}=2$ nm and 6 nm, respectively. The line is a guide to the eyes.

the critical angle θ_c (see below for definition).[26] Using these parameters, the strong uniaxial anisotropy ($H_k^{eff}>100$ Oe) can be obtained by assuming a preferential distribution of the easy axes of AF grains. Besides the enhancement of uniaxial anisotropy, it is of interest that the two-step magnetization process along the hard direction can also be successfully simulated. The mechanism of the two-step magnetization process is shown in Fig. 8. We also assume that $r=J_{F\text{-}AF}/(2K_{AF}t_{AF})>0.5$ to simulate the uniaxial nature. Thus, the surface moment of AF grains can switch following the rotation of the moment of the ferromagnetic layer. In the case of $0.5<r<1$, the surface moment of AF grains will follow the rotation of the ferromagnetic moment ($\mathbf{M}_F$) with a retardation and it is switching when $\mathbf{M}_F$ and the AED of the AF grain forms a critical angle (θ_c). During the switching process, the net surface moment flips irreversibly and the AED is reversed. The critical switching angle can be determined by the same astroid as that in Stoner-Wohlfarth model[27] in which the reduced external field is replaced by r, which gives

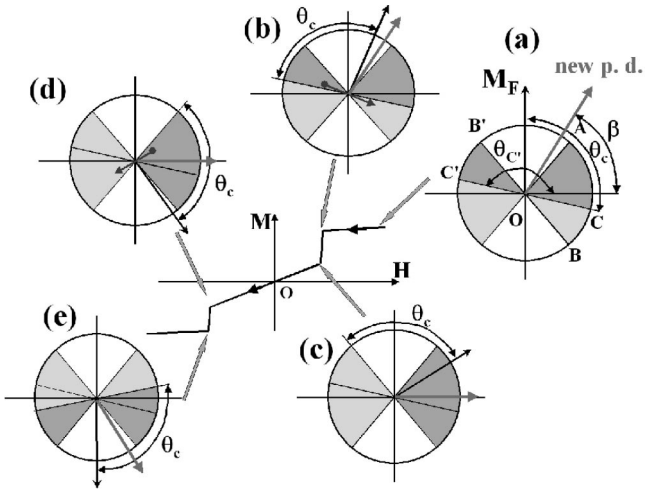

FIG. 8. Mechanism of two-step magnetization process. θ_c indicates the critical angle for switching, $\mathbf{M}_F$ the magnetic moment of the F layer, and new p.d. the new pinning direction.

$$r^{2/3}(\sin^{2/3}\theta_c+\cos^{2/3}\theta_c)=1. \quad (2)$$

We assume that, at the as-deposited state, all the AED's point to the right distributed between OA and OB as shown in Fig. 5(c) if an external magnetic field pointing to the right was applied during the sputtering process. If the hysteresis loop starts from the saturated state along the hard direction, $\mathbf{M}_F$ points to the hard direction with AED's distributed as shown in Fig. 8(a). The AED's, which make an angle with the direction of $\mathbf{M}_F$ (hard direction) larger than θ_c, flip into the left part, while the others (the major part) remain at the right part, resulting in a new distribution divided into two parts OC'-OB' and OA-OC, as shown in Fig. 8(a). A new pinning direction, which makes an angle β with the initial pinning direction, is determined by this new distribution of AED's of the AF grains. When the magnetic field is decreased, $\mathbf{M}_F$ rotates clockwise towards the new pinning direction [(a)→(b)]. This process is reversible and looks like a typical magnetization process along the hard direction, which is controlled by the torque balance between the contributions from the external field and the AF-F interlayer coupling. If the new pinning direction makes an angle larger than θ_c with some of the switched AED's on the left ($\theta_{C'}$-$\beta>\theta_c$), that is, if the angle between the new pinning direction and the hard direction ($\pi/2-\beta$) is larger than $2\theta_c-\pi$, those AED's will switch back from left to right when $\mathbf{M}_F$ rotates back toward the new pinning direction with the decrease of the applied field. The switching of AED's can induce further rotation of $\mathbf{M}_F$, which will, in turn, switch more AED's from left to right. This self-accelerating process causes a steep slope (i.e., a step) in the M-H curve [(b)→(c)]. This is either a reversible or irreversible process, depending on the r value, which stops when no more AED's can be switched due to a vacancy area in the easy-axis distribution around the hard direction, and is followed by a reversible rotation process with a less slope [(c)→(d)]. When $\mathbf{M}_F$ rotates to make θ_c with the AED, OA, another self-accelerating process starts with the switching of the AED from right to left [(d)→(e)], giving rise to the second step in the M-H curve. No flip of the AED occurs when $\theta_0/2<\pi-\theta_c$. Thus, the necessary condition for yielding the two-step magnetization process along the hard direction is $0<\theta_0<2(\pi-\theta_c)$.

Figure 9 shows the simulated magnetization curves along the hard direction for different AF layer thicknesses. One can see that the change of the characteristics of the magnetization process with increasing t_{AF} is in good agreement with the experimental results. In the case of very a thin AF layer, the AF surface moment can follow $\mathbf{M}_F$ without switching behavior (i.e., $\theta_c=\pi/2$), and no hysteresis appears even at the stepping part. However, at the beginning and the end of magnetization process, the moment rotates faster than in the middle of magnetization process. The faster parts are due to the change of the AED's. Here the AED's change via second-order transitions, not first-order transitions. With increasing t_{AF}, i.e., increasing the anisotropy per unit area of the AF grains, the first-order transition starts to occur in some of the AF grains, in two steps. With decreasing the field from the saturation in the positive hard direction, the spins of the AF

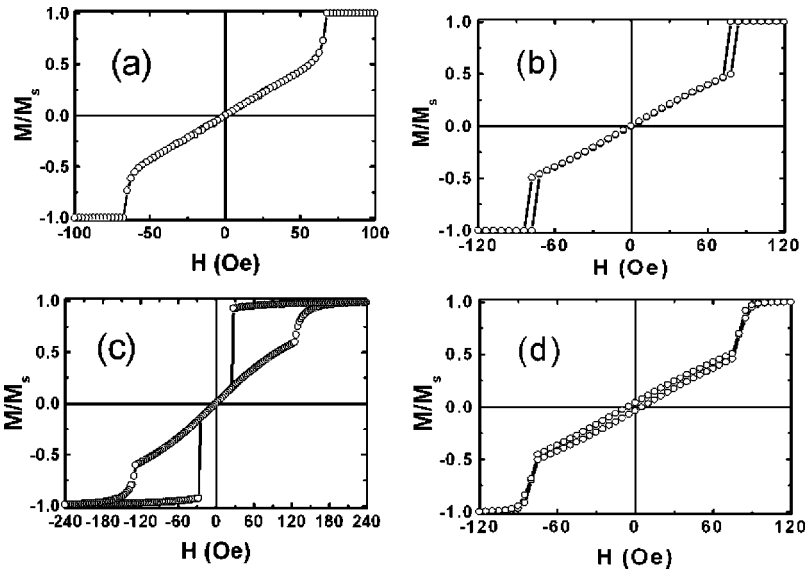

FIG. 9. Calculated hysteresis loops along hard direction with $J_{F\text{-}AF}/2K_{AF}t_{AF}=1.3$, 0.95, and 0.7 for (a), (b), and (c), respectively. The other parameters used in calculations are $J_{F\text{-}AF}=0.25$ erg/cm^2 and $\theta_0=\pi/3$. For (d), the same parameters as (b) are used and it is assumed that the local pinning directions uniformly disperse in a cone of 6°.

grains in the second quadrant first start to switch accompanied by the switching of their AED's into the fourth quadrant. Then at some negative field, some spins of the AF grains in the first quadrant start to switch and their AED's are switched to the third quadrant. It is obvious that a symmetric curve is obtained for increasing field. With the increase of t_{AF}, the first critical field on the descending curve decreases while the second critical field on the ascending curve increases. Similar features can also be observed on the experimental curves. However, some disagreements between the simulated and experimental curves are seen. According to the simulation, the remanence is zero if the first step happens before the field decreases to zero [see Fig. 9(b)]. This is not true for some experimental curves [see Fig. 4(b)]. To understand the nonzero remanence, we have to go beyond the coherent rotation model. One possible explanation is as follows: When the AF layer is relatively thin ($t_{NiO}\approx 4$ nm), i.e., $\theta_c\approx\pi/2$, the AED distribution at the saturated state along the hard direction is rather symmetrical with respect to the hard direction. When the field is removed, the local magnetic moments can rotate either clockwise or counterclockwise due to variation of local magnetic properties in AF and/or F layer. Then the entire area of the film can split into small parallel magnetic domains separated by Néel walls and give rise to a nonzero remanence.[28] Another explanation would be as follows: Instead of splitting into parallel domains, the ferromagnetic layer may be divided into many small regions,[29,30] inside which the magnetic moments are parallel to each other, but the direction of magnetization slightly changes from region to region due to the inhomogenous distribution of AF grains giving rise to a dispersion in the local pinning directions. Figure 9(d) demonstrates how a very small dispersion of the local pinning direction can result in the nonzero remanence along the hard direction.

As shown above, the mechanism of the two-step magnetization process and the enhanced uniaxial anisotropy can be well understood using a simplified picture of the preferential distribution, in which the easy axes of AF grains are assumed to uniformly distribute within a certain angle range around the pinning direction. A realistic preferential distribution would be that the probability for the AF easy axes distributing around the pinning direction is much larger than that around the hard direction, such as a modified Gaussian function with respect to the angle, which can give rise to the constant shift part of the nonvanishing rotational hysteresis while keeping the characteristics of the preferential distribution because a retardation angle between the F moment and the effective pinning exists in the whole angle range although the population of the AF spins being switched can be very different depending on the F moment orientation. The distribution function can be obtained by fitting the experimental curves if the distribution of the F/AF interfacial coupling has been estimated according to the grain size distribution or is set as a fitting parameter as well. The preferential distribution is evidently a rather general feature in the F/AF bilayers because the enhanced uniaxial anisotropy and the two-step magnetization process were also observed in many different types of bilayers, such as NiFe/IrMn [see Figs. 10(a) and 11(a)], CoFe/NiO [see Figs. 10(b) and 11(b)], CoFe/Fe_2O_3 (Ref. 31), NiFe/Fe_2O_3 (Ref. 31), and NiFe/FeMn (Ref. 32) when the AF layers are relatively thin. Assuming a preferential distribution, the coexistence of the unidirectional and uniaxial anisotropies in the bilayers with thick AF layers[33–35] can also be easily understood, although an alternative explanation has been proposed.[36,37] The model described above can be regarded as an extension of the FC-type model, which can account for all the phenomena that can be explained by the previous FC-type models[12–15] and also the new phenomena related to the preferential distribution of the easy axis of AF grains. Although the discussions in this paper are limited to the effect of the implantation of the preferential distibution into the FC-type models for the polycrystalline F/AF bilayers, the concept of a preferential distribution could be also introduced into other types of models, resulting in similar or even more complicated phenomena.

Although the observed phenomena can be well described by the preferential distribution of the easy axes of the AF grains, the origin of such a distribution is still an open question. To our knowledge, there could be several reasons: (1)

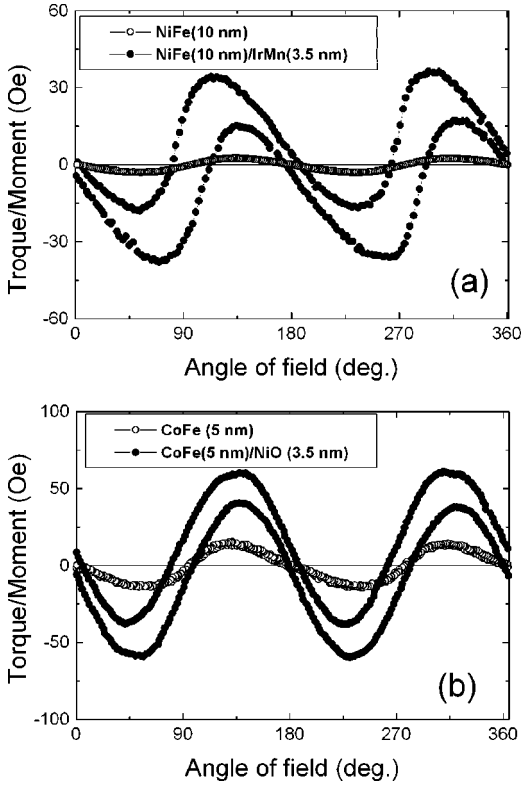

FIG. 10. Torque curves of (a) NiFe (10 nm) and NiFe (10 nm)/IrMn (3.5 nm) and (b) CoFe (5 nm) and CoFe (5 nm)/NiO (3.5 nm) measured in magnetic fields high enough to saturate the sample. The torques have been normalized with respect to the magnetic moment of the sample which can be deduced from torque amplitude at low field. NiFe/IrMn and CoFe/NiO layers show strongly enhanced uniaxial anisotropy compared with the single ferromagnetic layers of NiFe and CoFe, respectively.

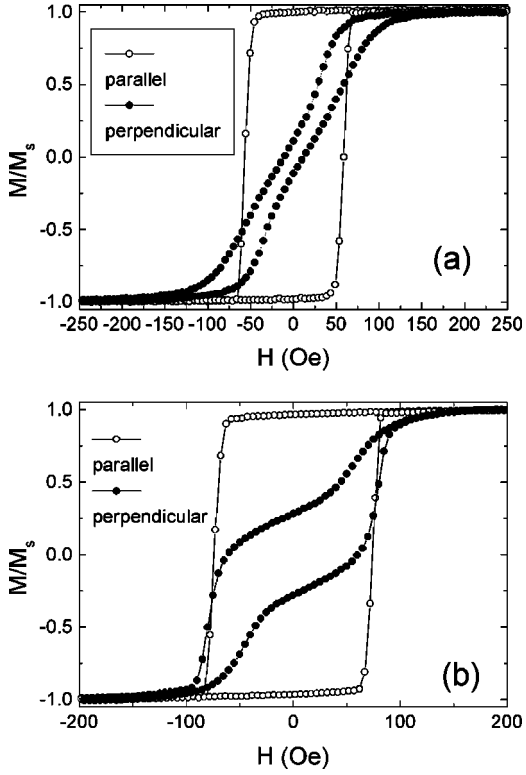

FIG. 11. Hysteresis loops of (a) NiFe (10 nm)/IrMn (3.5 nm) and (b) CoFe (5 nm)/NiO (3.5 nm) bilayers measured along both the easy and hard directions. The two-step magnetization processes can be seen on the hard-axis loops.

The in-plane texture structure can give rise to a preferential distribution of the easy axis of the crystalline anisotropy of the AF grains. In our samples, a combined (111) and (200) out-plane texture was observed, but no in-plane texture was detected by x-ray diffraction. High-resolution transmission electron microscopy (TEM) would be of help in tracing the fine structures. (2) In-plane anisotropic stress may cause a preferentially distributed magnetoelastic anisotropy. The in-plane anisotropic stress may originate from a combination of the magnetostriction of the magnetic layer, the different thermal expansion coefficients of different materials, and the interfacial lattice matching if the magnetic film is deposited under an external field.[38,39] To quantify the anisotropy caused by the stress, one needs information about the stress distribution in the NiO layer and the magnetostriction constant of the NiO film. (3) A preferential distribution of the strength of the interfacial coupling may be phenomenologically equivalent to the preferential distribution of the AF easy axes. During the preparation or annealing under an external field, the net moment at the surface of NiO may increase through the diffusion of the interfacial atoms to minimize the interfacial exchange energy.[40] For example, if the easy axis of the AF grain is parallel to the applied field direction and a ferromagnetic coupling between the F moment and the AF spin is assumed, the local atomic spins at the surface of the AF grain can be either parallel or antiparallel to the F moment. The atoms at the interface tend to rearrange by diffusion so that more interfacial atomic spins orientate parallel to the F moment. The driving force, the F/AF exchange energy, is proportional to the cosine of the angle between the F moment and the atomic spin of NiO, which is determined by the easy direction of the AF grain and the r value. It can be deduced that the AF grain with its easy axis along the applied field direction has the largest increase of the surface net moment and gives rise to a preferential distribution of the interfacial exchange coupling. This distribution should be sensitive to the thickness of the AF layer because of the variation of the r value. The phenomena we observed may come from a kind of combination of the mechanisms described above. Further investigations of the interface structure, stress distribution, and magnetic annealing effect are required to clarify the mechanism and to provide useful information about the nature of the anisotropy and the interfacial coupling in the bilayers.

In conclusion, the enhanced uniaxial anisotropy and the two-step magnetization process in the NiFe/NiO bilayers can be well explained by the preferential distribution of the easy axes of the AF grains. The preferential distribution model can serve as a more realistic model for polycrystalline F/AF bilayers than the parallel alignment, which cannot explain the two-step magnetization process and nonvanishing rotational hysteresis at high field, or the random distribution model, which cannot account for the enhanced uniaxial an-

isotropy and the two-step magnetization process. It was made clear that knowledge of the distribution of the AF easy axes is essential for understanding both the characteristics and the amplitude of the effective anisotropy of the bilayers. Further studies of the origin of the preferential distribution will be valuable in revealing the nature of the exchange-coupled F/AF bilayers.

ACKNOWLEDGMENTS

This work was supported by the DOD-ARO (Grant No. DAAH04-96-1-0316) and made use of the NSF MRSEC Shared Facilities (Grant No. 542417-55139). The authors wish to thank F. Huang and Dr. J. Barnard for their helpful discussions about the stress measurement.

[1] W.H. Meiklejohn and C.P. Bean, Phys. Rev. **102**, 1413 (1956); **105**, 904 (1957).

[2] For recent reviews see J. Nogues and I.K. Schuller, J. Magn. Magn. Mater. **192**, 204 (1999); A.E. Berkowitz and K. Takano, *ibid.* **200**, 552 (1999).

[3] D. Dieny, V.S. Speriosu, S.S.P. Parkin, B.A. Gurney, D.R. Wilhoit, and D. Mauri, Phys. Rev. B **43**, 1297 (1991).

[4] A.P. Malozemoff, Phys. Rev. B **35**, 3679 (1987); **37**, 7673 (1988).

[5] N.C. Koon, Phys. Rev. Lett. **78**, 4865 (1997).

[6] D. Mauri, H.C. Siegmann, P.S. Bagus, and E. Kay, J. Appl. Phys. **62**, 2047 (1987).

[7] T.C. Schulthess and W.H. Butler, Phys. Rev. Lett. **81**, 4516 (1998).

[8] K. Takano, R.H. Kodama, A.E. Berkowitz, W. Cao, and G. Thomas, Phys. Rev. Lett. **79**, 1130 (1997).

[9] F.Y. Yang and C.L. Chien, Phys. Rev. Lett. **85**, 2597 (2000).

[10] L. Néel, Ann. Phys. (N.Y.) **2**, 61 (1967).

[11] H. Fujiwara and M. Sun, J. Appl. Phys. **85**, 4940 (1997).

[12] E. Fulcomer and S.H. Charap, J. Appl. Phys. **43**, 4190 (1972).

[13] M.D. Stiles and R.D. Mc Michael Phys. Rev. B **60**, 12 950 (1999).

[14] C. Hou, H. Fujiwara, and F. Ueda, J. Magn. Magn. Mater. **198-199**, 450 (1999).

[15] H. Fujiwara, C. Hou, M. Sun, and H.S. Cho, IEEE Trans. Magn. **MAG-35**, 3082 (1999).

[16] R.D. McMichael, M.D. Stiles, P.J. Chen, and W.F. Egelhoff, Phys. Rev. B **58**, 8605 (1998).

[17] H.D. Chopra, D.X. Yang, P.J. Chen, H.J. Brown, L.J. Swatzendruber, and W.F. Egelhoff, Phys. Rev. B **61**, 15 312 (2000).

[18] P.J. Flanders and G. Wu, Rev. Sci. Instrum. **70**, 2732 (1999).

[19] M. Kowalewski *et al.*, J. Appl. Phys. **87**, 5732 (2000).

[20] C. Lai, H. Matsuyama, R.L. White, T.C. Anthony, and G.G. Bush, J. Appl. Phys. **79**, 6389 (1996).

[21] H. Xi and R.M. White, Phys. Rev. B **61**, 80 (2000).

[22] Y.J. Tang, X. Zhou, X. Chen, B.Q. Liang, and W.S. Zhan, J. Appl. Phys. **88**, 2054 (2000).

[23] R.P. Michel, A. Chaiken, C.T. Wang, and L.E. Johnson, Phys. Rev. B **58**, 8566 (1998).

[24] A. Fernandez and C.J. Cerjan, J. Appl. Phys. **87**, 1395 (2000).

[25] E. Girgis, J. Schelten, J. Shi, J. Janesky, S. Tehrani, and H. Goronkin, Appl. Phys. Lett. **76**, 3780 (2000).

[26] T. Zhao, K. Zhang, and H. Fujiwara, J. Appl. Phys. **89**, 7549 (2001).

[27] For instance, see G. Bertotti, *Hysteresis in Magnetism* (Academic Press, London, 1998).

[28] For instance, see A. Hubert and Schafer, *Magnetic Domains* (Springer-Verlag, Berlin, 1998).

[29] Z. Li and S. Zhang, Appl. Phys. Lett. **77**, 423 (2000).

[30] J. Yu, A.D. Kent, and S.S.P. Parkin, J. Appl. Phys. **87**, 5049 (2000).

[31] K. Zhang *et al.* (unpublished).

[32] X.M. Liu *et al.* (unpublished).

[33] T. Ambrose, R.L. Sommer, and C.L. Chien, Phys. Rev. B **56**, 83 (1997).

[34] T. Ambrose, R.L. Sommer, and C.L. Chien, J. Magn. Magn. Mater. **177-181**, 1235 (1998).

[35] Z. Qian, J.M. Sivertsen, and J.H. Judy, J. Appl. Phys. **83**, 6825 (1998).

[36] The coexistence of uniaxial and unidirectional anisotropy in bilayers with thick AF layers was ascribed to the complicated domain process during which the pinned AF grains break the symmetry of random distribution in Ref. 37. However, this cannot explain the uniaxial nature for bilayers with thin AF layers since there are no pinned AF grains to break the symmetry.

[37] M.D. Stiles and R.D. McMichael, Phys. Rev. B **63**, 064405 (2001).

[38] S.H. Lim, S.H. Han, H.J. Kim, S.H. Song, and D. Lee, J. Appl. Phys. **87**, 5801 (2000).

[39] We measured stresses in single layers of NiFe (20 nm) and NiO (10 nm) deposited on Si wafers (180 μm) under a magnetic field, by comparing the curvature of the wafer before and after the sputtering. It shows an anisotropic stress in NiFe film, 370 MPa and 690 MPa along the directions perpendicular and parallel to the applied field, respectively, and an isotropic stress of about -2150 MPa in NiO film.

[40] C. Hou, Ph.D. thesis, The University of Alabama, 1999.